International Journal of ENGINE RESEARCH

Standard Article

International J of Engine Research
1–15

DOI: 10.1177/1468087418767225
journals.sagepub.com/home/jer
SAGE

Optimization of multiple heat releases in pre-mixed diesel engine combustion for high thermal efficiency and low combustion noise by a genetic-based algorithm method

Gen Shibata[1], Hideyuki Ogawa[1], Yasumasa Amanuma[1] and Yuki Okamoto[2]

Abstract

The reduction of diesel combustion noise by multiple fuel injections maintaining high indicated thermal efficiency is an object of the research reported in this article. There are two aspects of multiple fuel injection effects on combustion noise reduction. One is the reduction of the maximum rate of pressure rise in each combustion, and the other is the noise reduction effects by the noise canceling spike combustion. The engine employed in the simulations and experiments is a supercharged, single-cylinder direct-injection diesel engine, with a high pressure common rail fuel injection system. Simulations to calculate the combustion noise and indicated thermal efficiency from the approximated heat release by Wiebe functions were developed. In two-stage high temperature heat release combustion, the combustion noise can be reduced; however, the combustion noise in amplification frequencies must be reduced to achieve further combustion noise reduction, and an additional heat release was added ahead of the two-stage high temperature heat release combustion in Test 1. The simulations of the resulting three-stage high temperature heat release combustion were conducted by changing the heating value of the first heat release. In Test 2 where the optimum heat release shape for low combustion noise and high indicated thermal efficiency was investigated and the role of each of the heat releases in the three-stage high temperature heat release combustion was discussed. In Test 3, a genetic-based algorithm method was introduced to avoid the time-consuming loss and great care in preparing the calculations in Test 2, and the optimum heat release shape and frequency characteristics for combustion noise by the genetic-based algorithm method were speedily calculated. The heat release occurs after the top dead center, and the indicated thermal efficiency and overall combustion noise were 50.5% and 86.4 dBA, respectively. Furthermore, the optimum number of fuel injections and heat release shape of multiple fuel injections to achieve lower combustion noise while maintaining the higher indicated thermal efficiency were calculated in Test 4. The results suggest that the constant pressure combustion after the top dead center by multiple fuel injections is the better way to lower combustion noise; however, the excess fuel injected leads to a lower indicated thermal efficiency because the degree of constant volume becomes deteriorates.

Keywords

Diesel combustion, combustion noise reduction, thermal efficiency, optimization of heat release shape, multiple fuel injections, genetic-based algorithm method

Date received: 14 September 2017; accepted: 24 February 2018

Introduction

In diesel engines, much combustion noise is generated with high indicated thermal efficiencies and it makes difficult to achieve the premixed diesel combustion at high load. There are several reports of combustion noise reduction of diesel engines. Murayama et al.[1] investigated the combustion noise caused by the

[1]Division of Energy and Environmental Systems, Hokkaido University, Sapporo, Japan
[2]Yanmā Kabushiki-Gaisha, Osaka, Japan

Corresponding author:
Gen Shibata, Division of Energy and Environmental Systems, Hokkaido University, North-13, West-8, Kita-ku, Sapporo 060-8628, Hokkaido, Japan.
Email: g-shibata@eng.hokudai.ac.jp

burning rate, and Kojima[2] explained the mechanism of combustion noise generation. Komori et al.[3] succeeded in distinguishing the combustion and the engine noise components and developed a basic model for combustion noise simulation. Sjoberg and Dec[4] and Johansson et al.[5] suggested ringing intensity control, and the relation between combustion noise and pressure history was reported by Scarpati et al.[6] and Shahlari et al.[7] The maximum rate of pressure rise is a main cause of the combustion noise, and Shibata et al.[8] investigated other factors in combustion noise generation. A total of 18 engine tests were conducted at one maximum rate of pressure rise condition (1.0 MPa/CA), and it was statistically determined that the maximum rate of heat release and the crank angle of the 50% burn are the second and third most influential parameters in the combustion noise. Ozawa and Nakajima[9,10] investigated the simultaneous improvement of combustion noise and fuel consumption and tried to control the combustion chamber resonance of a diesel engine.

The combustion noise simulation method by coherence analysis was developed by Okubo and Yonezawa.[11] Shibata et al.[12,13] improved this simulation technique using the Wiebe function and were able to predict combustion noise for multiple fuel injections. In 2014, Fuyuto et al.[14] reported "Noise Canceling Spike Combustion (NCS combustion)": here the combustion noise generated in the second combustion assists in reducing the combustion noise of the first fuel injection. (The details of the NCS combustion are described in Appendix 1.) Ikeda and colleagues[15,16] investigated the feasibility and possibility of controlling the two-peak heat release rate during the high temperature heat release (HTHR) by numerical calculations with single- and two-zone models of CHEMKIN PRO; however, the calculated results did not explain the NCS combustion well. Shibata and colleagues[17,18] developed combustion noise simulation further and applied it to two-stage HTHR NCS combustion in 2016 and discussed the NCS combustion mechanism. Furthermore, Busch et al.[19,20] reported the combustion noise reduction by short pilot-main injections and much research has been conducted with combustion noise spectrum analysis. The fuel penetration rate data provide evidence that rate shaping of the initial phase of the main injection is occurring in the engine and that this rate shaping is largely consistent with the injection rate data; however, the results demonstrate that these changes are not directly responsible for the observed trends in combustion noise. Fuyuto and Taki[21] reported details of the theory of NCS combustion for the $dP/d\theta$ peak of a pilot and a single $dP/d\theta$ peak of the main combustion relatively, using experimental data analysis and zero-dimensional cycle simulations. As detailed above, combustion noise research has been conducted both with simulations and engine tests; however, the combustion noise in the amplification frequencies must be reduced to achieve further combustion noise reductions.

Table 1. Test engine specifications.

Number of cylinders	1
Bore × Stroke (mm)	ϕ 85.0 × 96.9
Stroke volume (cm^3)	550
Compression ratio	16.3:1
Fuel injection system	Common rail
Nozzle hole	ϕ 0.125 × 7
Spray angle (°)	156
Connecting rod/crank radius ratio	L/R = 3.1

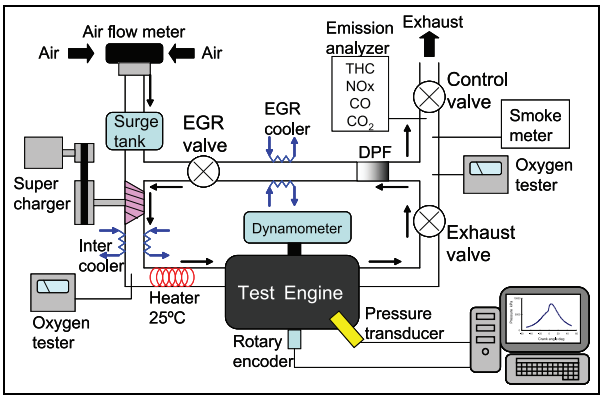

Figure 1. Outline of the engine test set-up.

In this article, the effects of multiple fuel injections more than three times on further combustion noise reduction maintaining the higher indicated thermal efficiency were investigated by combustion noise simulations and engine tests. Furthermore, a genetic-based algorithm (GA) method was introduced, and the optimum number of fuel injections and heat release shapes for lower combustion noise, maintaining the higher indicated thermal efficiency were calculated and discussed.

Experimental

Engine bench set-up

The engine employed in the experiments was a supercharged, single-cylinder direct-injection (DI) diesel research engine with a common rail fuel injection system for injection pressures up to 180 MPa. The specifications of the engine are given in Table 1 and the fuel used in the experiments was the commercially available #2 Japanese diesel fuel (54 CN). The outline of the engine bench set-up is shown in Figure 1. The intake air was measured by an orifice flow meter and mixed with low pressure cooled exhaust gas recirculation (EGR) gas boosted by a supercharger, before being supplied to the engine. The intake air temperature was maintained at 25 °C by an electric heater in the intake manifold. The in-cylinder pressure data were measured by a pressure transducer (Kisler 6125A) and the 45 crank angle resolved pressure data were recorded on a PC. For all test conditions here, the cooling water and engine oil temperatures were maintained at 80 °C.

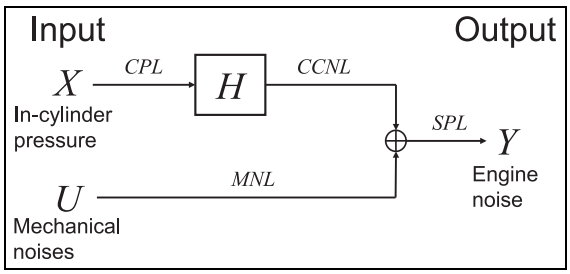

Figure 2. Engine noise generation and analysis model.

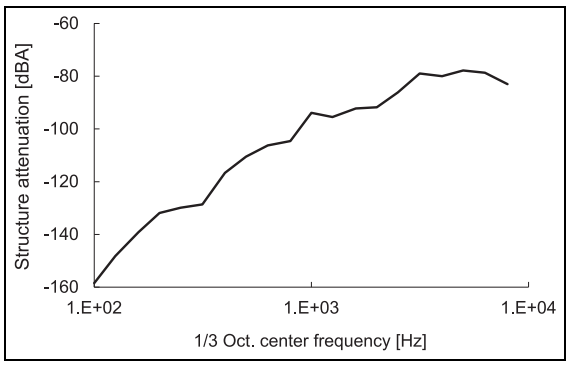

Figure 3. Structural attenuation of the test engine.

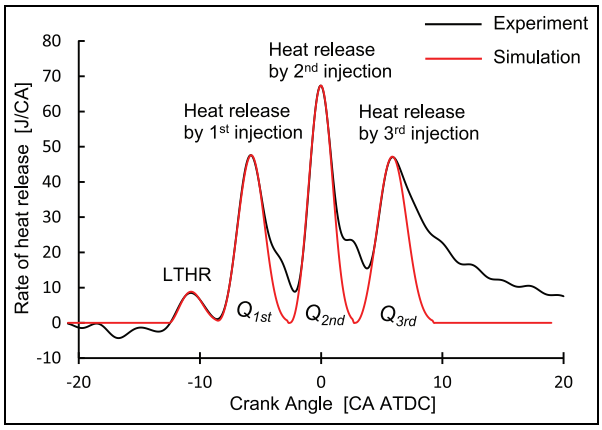

Figure 4. Approximation by the Wiebe function for the three-stage HTHR combustion.

Engine experiments were conducted to calculate the structure attenuation (SA) of the test engine, as in Figure 3 and evaluate the accuracy of the simulation, as shown in Figures 5 and 6.

Noise measurements and calculations

Measurements of the engine noise. The engine and combustion noise were evaluated with the noise measurement arrangement. The supercharger at the right is surrounded by acoustic absorption panels and materials, and microphones were set at two sampling positions at the cylinder head top height (the one 1 m away from the front of the engine and the other 1 m to the

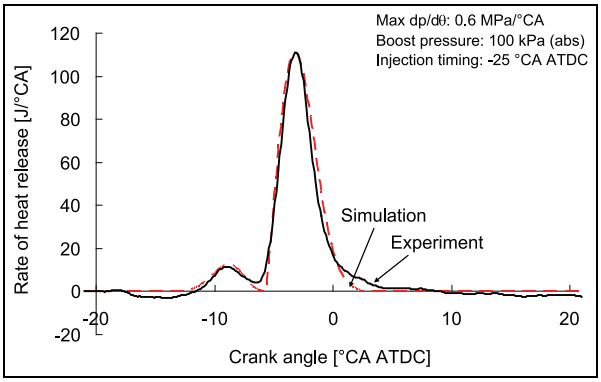

Figure 5. Heat release data in the engine experiment and simulation.

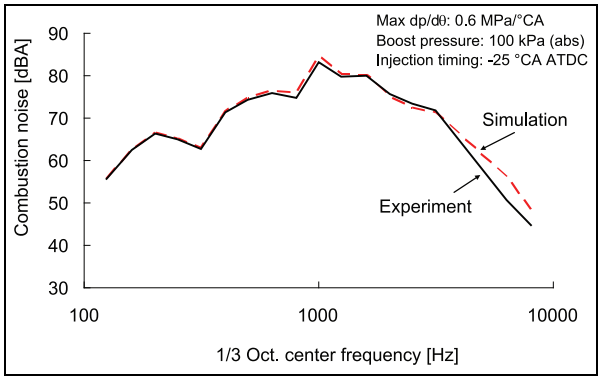

Figure 6. Plots of the combustion noise in the engine experiment and simulation.

left of the engine) and engine noise was recorded from the left and front of the engine, avoiding the noise from the transmission at the rear of the engine. The sampled noise was averaged and analyzed by fast Fourier transformation (FFT) sound analyzers (Onosokki LA-1410 and DS-3000) and a 1/3 octave band filter was used for the analysis of the frequency characteristics.

Calculations of combustion noise. The model used to analyze the engine noise is outlined in Figure 2. The engine noise value comprises the combustion noise level by the coherence method (CCNL) and the mechanical noise level (MNL) as shown in equation (1), here assuming that the cylinder pressure and combustion noise levels are closely related. The transfer characteristic H was calculated from the power spectrum by the FFT analysis of the in-cylinder pressure waveform and the cross spectrum of the sound pressure of the engine noise level and pressure waveform. With this, the coherence combustion noise level (CCNL) is calculated from the in-cylinder pressure level (CPL) and the transfer characteristics H by equation (2).

The pressure changes generate vibrations, transfer, and attenuate in the cylinder block, before release from the surface of the engine as combustion noise. The

frequency characteristics are specific to the engine used. The engine SA can be calculated from the coherence combustion noise level and CPL by equation (3), it was calculated under several conditions and averaged to provide a representative SA curve. Figure 3 shows the frequency characteristics of the SA of the test engine, and the combustion noise level (CNL) in the engine tests and simulations are calculated from the CPL and the SA by equation (4). (The direct noise measurements are conducted to determine the engine transfer function H. Once the SA is obtained, the combustion noise is calculated by equation (4))

$$SPL = CCNL + MNL \tag{1}$$

$$CCNL = CPL * H \tag{2}$$

$$SA = CCNL - CPL \tag{3}$$

$$CNL = SA + CPL \tag{4}$$

where SPL is the sound pressure level (dBA), CCNL is the combustion noise level by coherent method (dBA), MNL is the mechanical nose level (dBA), H is the transfer characteristic, SA is the structure attenuation (dBA), CNL is the combustion noise level (dBA), and CPL is the cylinder pressure level (dBA).

The sensitivity of the human ear changes depending on the frequency range and the "A" weighted sound pressure level, the dBA, was used to evaluate the perceived loudness of the overall combustion noise (OA).

Simulation methods. Methods of combustion noise simulation for three-stage HTHR combustion. An example of the heat release shape in three-stage HTHR combustion is shown in Figure 4. The heat release history was synthesized by introducing the Wiebe function in equation (5) four times; one time for the low temperature heat release (LTHR) and one each for the first, second, and third HTHRs. The in-cylinder pressure history was calculated from the heat release history by the Runge–Kutta numerical method in equation (6), and the kappa is calculated for every 0.20 crank angle from the in-cylinder temperature and the cylinder gas composition. The OA and frequency characteristics of the combustion noise were calculated from the frequency characteristics of the in-cylinder pressure by Fourier transformation and the structural attenuation.

In Test 2, the Wiebe functions were fitted to the heat release history of three-stage HTHR combustion in the engine test and the parameters M and combustion duration (θ_z) in Table 2 were obtained and used for each of the heat release calculations. Then, the OA and frequency characteristics of the combustion noise were calculated

$$\frac{dQ}{d\theta} = 6.9 \cdot \frac{Q_{total}}{\theta_z} \cdot (M+1) \cdot \left(\frac{\theta}{\theta_z}\right)^{M} \cdot \exp\left\{-6.9 \cdot \left(\frac{\theta}{\theta_z}\right)^{M+1}\right\} \tag{5}$$

Table 2. Values of parameters M and θ_z in the Wiebe function for Q_{1st}, Q_{2nd}, and Q_{3rd} in the three-stage HTHR combustion (Test 2 and Test 3).

	LTHR	Q_{1st}	Q_{2nd}	Q_{3rd}
M	1.5	2.15	2.2	2.1
θ_z	4.7	5.9	5.3	6.5

LTHR: low temperature heat release.

where Q_{total} is the total heat release (J), θ_z is the combustion duration (CA), M is the parameter, and θ is the crank angle (CA)

$$\frac{dP}{d\theta} = \frac{\kappa - 1}{V} \cdot \frac{dQ}{d\theta} - \kappa \cdot \frac{P}{V} \cdot \frac{dV}{d\theta} \tag{6}$$

where Q is the heat release (J), κ is the ratio of specific heats, P is the pressure (Pa), V is the volume (m3), and θ is the crank angle (CA).

Evaluation of the adequacy of the combustion noise simulation. The combustion data obtained by engine test experiments and simulations were compared to evaluate the accuracy of the combustion noise simulation. The heat release history of the engine data and the approximated history of the heat release by the Wiebe function are plotted together in Figure 5, and the combustion noise data of the experiment and simulation at 100–8000 Hz are plotted in Figure 6. The frequency characteristics of the simulation were very similar to the experiments, verifying that the combustion noise could be evaluated by the simulation.

GA method. To calculate the optimum number of fuel injections and heat release shape in multiple fuel injections to achieve lower combustion noise maintaining the higher indicated thermal efficiency, the GA method was introduced. The GA method is an application of the evolution process with mutations and crossovers of organisms, where the calculated results approach the optimum solution as the number of generations increase. The GA method is effective in situations where parameters are intricately interrelated and is introduced here to optimize the heat release shapes of the multiple fuel injections.

In the GA method, the result approaches the exact solution with increasing number of generations, and the calculations are continued until the result does not change over 100 generations, and the result of the final generation is considered the answer for the GA method. Equation (7) shows an example of the evaluation function for the GA method used in the research here. When the indicated thermal efficiency is high and the OA is low, the score becomes high, and the equation defined as the 0.5% indicated thermal efficiency is equivalent to 1.0 dBA of OA. (The details of the optimum number of generations and the evaluation function are described in Appendix 2)

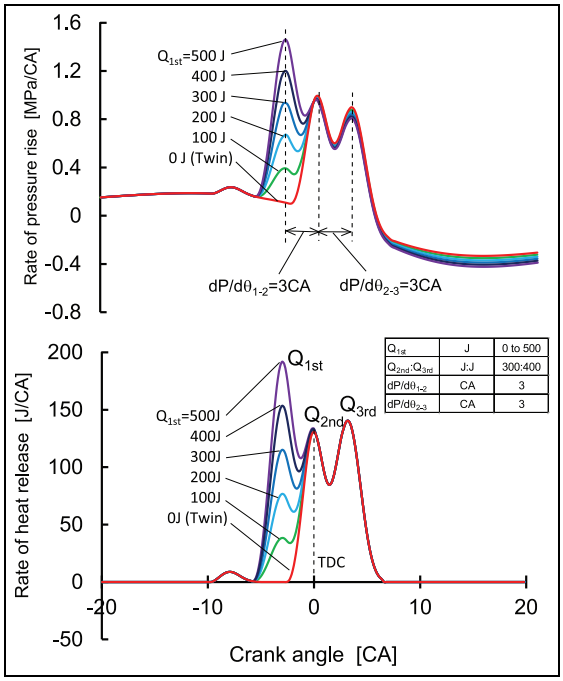

Figure 7. Combustion noise reduction method in three-stage HTHR combustion (Test 1).

$$Score = \eta i - OA \cdot 0.5 \tag{7}$$

where *Score* is the score of evaluation function, ηi is the indicated thermal efficiency (%), and OA is the overall combustion noise (dBA).

Test conditions for simulations. The initial conditions of the simulations were set to a 15.0% intake oxygen concentration, an engine speed of 2000 r/min, and a 150 kPa (abs) boost pressure. To investigate the mechanism of multiple fuel injections in the reduction of combustion noise, a three-stage HTHR combustion near the top dead center (TDC) was attempted by the combustion noise simulation in Test 1. The red curve in Figure 7 shows the optimum heat release shape for low combustion noise with high indicated thermal efficiency in two-stage HTHR combustion,[17] and an additional heat release was added ahead of the optimum two-stage HTHR combustion. Then, the optimum heat release shape in the three-stage HTHR combustion was obtained in Test 2 and validated separately by the GA in Test 3. Following this, the number of fuel injections was increased, and an optimum number of fuel injections and heat release shapes for lower combustion noise maintaining the higher indicated thermal efficiency were investigated by the GA method in Test 4.

Test 1: mechanism of combustion noise reduction by three-stage HTHR combustion. For the two-stage HTHR combustion simulation, the crank angle of the peak heat release in the first fuel injection was set at TDC and the heating values of the first and second heat releases and the position of the second heat release were changed as variable parameters. The red curve in Figure 7 shows the optimum heat release shape for the two-stage HTHR combustion calculated by the simulation.[17] A further heat release was added ahead of the optimum two-stage HTHR combustion and the effects of this three-stage HTHR combustion on combustion noise reduction were simulated. As shown in Figure 7, the heating value of the first heat release is a parameter variable varied from 100 to 500 J, and the $dP/d\theta_{1-2}$ and $dP/d\theta_{2-3}$ maintained to be 3 CA.

Test 2: optimization of the heat release shape for low combustion noise and high indicated thermal efficiency in three-stage HTHR combustion. To aim for higher degree of constant volume combustion, the peaks of the first, second, and third combustions were located before TDC, at TDC, and after TDC, respectively, and the optimum heat release shape for a higher indicated thermal efficiency with low combustion noise was calculated in Test 2. The total heat release was maintained at 604 J, including 19 J of LTHR. In each of the heat releases, the parameter M and θ_z in the Wiebe functions were the same as shown in Table 2. The parameter variables in the simulations were as follows:

1. The length of time in crank angle between the peaks of the rate of pressure rise in Peaks 1 and 2 ($dP/d\theta_{1-2}$) was varied from 3 to 5 CA in 1 CA steps.
2. The length of time in crank angle between the peaks of the rate of pressure rise in Peaks 2 and 3 ($dP/d\theta_{2-3}$) was varied from 3 to 7 CA in 1 CA steps.
3. The heating values for the Q_{1st}, Q_{2nd}, and Q_{3rd}
   (a) The total amount of Q_{1st}, Q_{2nd}, and Q_{3rd} is 585 J.
   (b) The Q_{1st} value was varied from 75 to 435 J in 40 J steps.
   (c) The Q_{2nd} value was varied from 75 to 275 J in 40 J steps.
   (d) The Q_{3rd} value was 585 J minus the sum of the Q_{1st} and Q_{2nd} values

($Q_{3rd} = 585 - Q_{1st} - Q_{2nd}$ and $Q_{3rd} \geqslant 75$J)

The appearance and details of the heat release parameters in the three-stage HTHR combustion are shown in Figure 8.

Test 3: introduction of the GA method to validate the optimized heat release shape of three-stage HTHR combustion in Test 2. The optimum heat release shape in the three-stage HTHR combustion was obtained in Test 2 and validated separately by the GA method in Test 3. Equation (7) (above) was used as the evaluation function. The calculation was conducted until the score does not change over 100 generations and the calculated result of the final generation was considered the

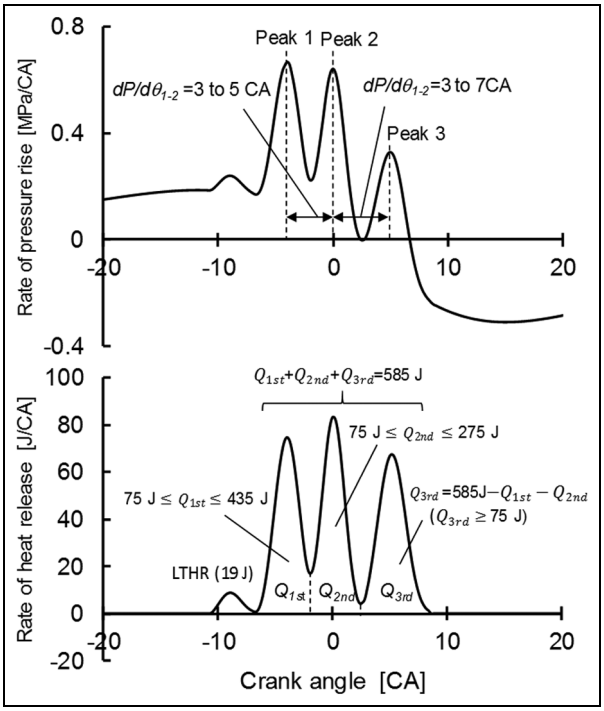

Figure 8. Variable parameters in the calculations for Tests 2 and 3.

answer of the GA method. In the calculations, a random number is used and introduced in some calculations to avoid generating a local non-optimal solution. In each of the heat releases, the parameters M and θ_z in the Wiebe functions were the same as shown in Table 2. The parameter variables in the GA method here were set as follows:

1. Three fuel injections.
2. The crank angle positions of peak heat releases for the LTHR, Q_{1st}, Q_{2nd}, and Q_{3rd} were changed within the range from −30 to 40 CA after top dead center (ATDC) in 0.1 CA steps.
3. The combustion duration for each heat release was changed from 4 to 10 CA in 0.1 CA steps.
4. The heating value of the LTHR was maintained at 19 J.
5. The heating values for the Q_{1st}, Q_{2nd}, and Q_{3rd} were changed from 0 to 585 J in 0.1 J steps; however, the total amount of Q_{1st}, Q_{2nd}, and Q_{3rd} is everywhere 585 J.

Test 4: optimum number of fuel injections and heat release shapes for lower combustion noise with high indicated thermal efficiency analyzed by the GA method. The combustion noise decreases with an increasing number of fuel injections; however, the indicated thermal efficiency decreases because the degree of constant volume worsens. In Test 4, the combustion noise and indicated thermal efficiency versus number of fuel injections were investigated by the GA method, and the optimum number of fuel injections was determined. The number

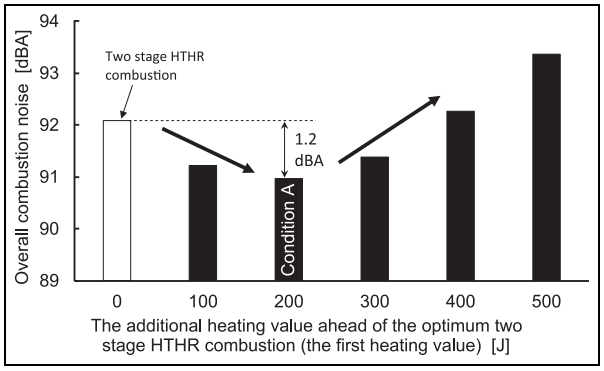

Figure 9. Overall combustion noise versus the additional heating value added ahead of the two-stage HTHR combustion.

of fuel injections was changed from one to five and the crank angle positions of peak heat releases and heating values were used as parameter variables:

1. Multiple fuel injections: the number of fuel injections is 1 to 5.
2. The M parameter in the Wiebe function in each of the combustions is 2.0.
3. The crank angle positions of the peak heat releases for the LTHR, Q_{1st}, Q_{2nd}, Q_{3rd}, Q_{4th}, and Q_{5th} were changed within the −30 to 40 CA ATDC range in 0.1 CA steps.
4. The combustion duration for each heat release was varied from 4 to 10 CA in 0.1 CA steps.
5. The heating value of the LTHR was maintained at 19 J.
6. The heating values for Q_{1st}, Q_{2nd}, Q_{3rd}, Q_{4th}, and Q_{5th} were changed from 0 to 585 J in 0.1 J steps, with the total of Q_{1st}, Q_{2nd}, Q_{3rd}, Q_{4th}, and Q_{5th} as 585 J.

Results and discussion

Test 1: mechanism of combustion noise reduction by three-stage HTHR combustion

For the three-stage HTHR combustion, one heat release was added ahead of the two-stage HTHR combustion with the low engine noise and high indicated thermal efficiency at the optimum,[17] and the heating value of the first heat release was varied from 100 to 500 J, as shown in Figure 7. Figure 9 plots the OA versus the additional heating value added ahead of the two-stage HTHR combustion. When the first heating value is 200 J (condition A in Figure 9), the OA is 1.2 dBA lower than that of the two-stage HTHR combustion (the 0 J case), and OA increases with increases in the first heating value above 200 J. Figure 10(a) shows the heat release shape and the rate of pressure rise in condition A. The three-stage HTHR heat release in Figure 10(a) was disassembled into three sets of two-stage heat releases, the Twin_{1-2}, Twin_{1-3}, and Twin_{2-3}, to investigate the reduction and amplifying

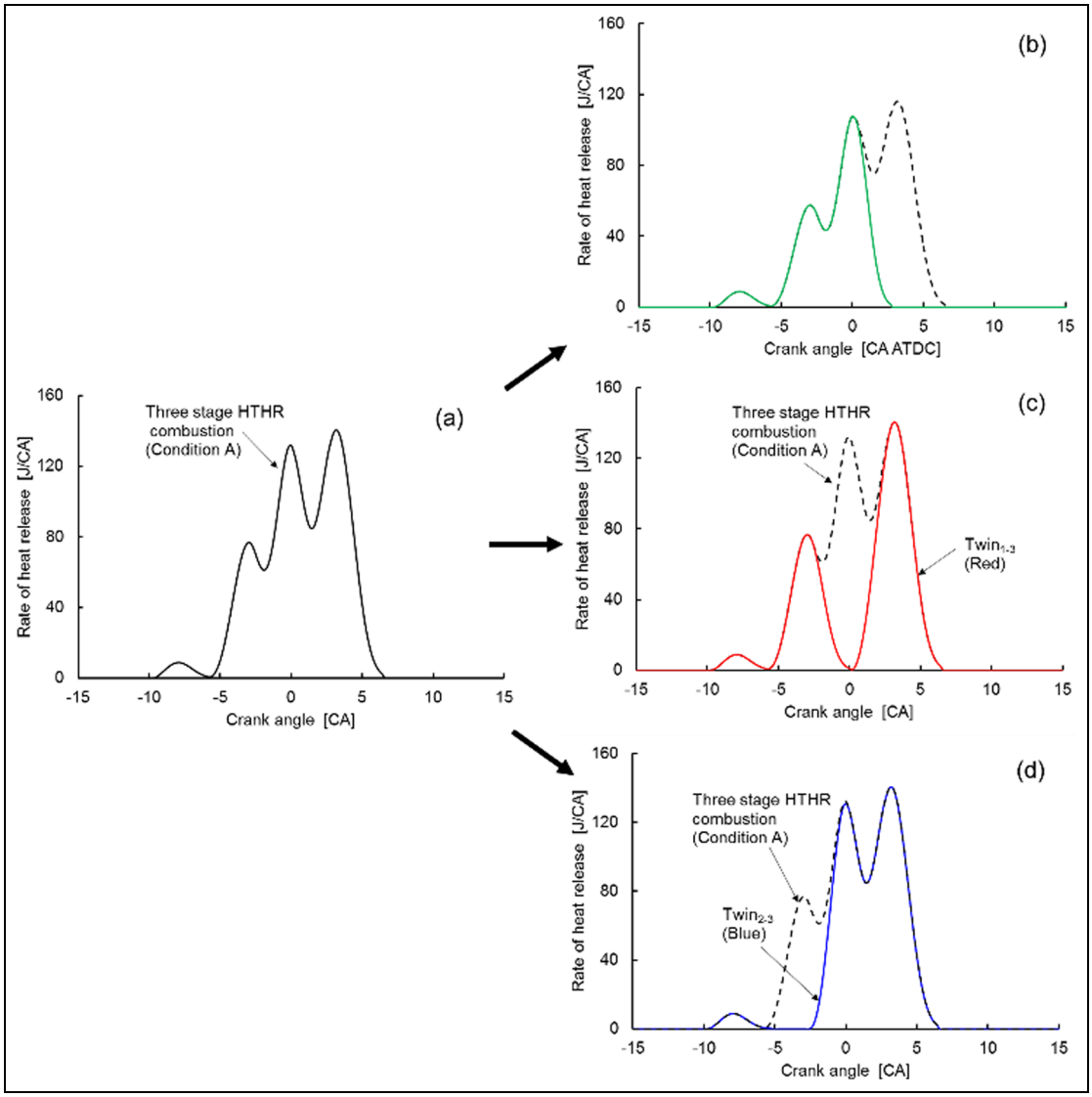

Figure 10. The optimum heat release shape for the three-stage HTHR combustion in Test 2: (a) three-stage HTHR release, (b) $Twin_{1-2}$, (c) $Twin_{1-3}$, and (d) $Twin_{2-3}$.

frequencies of combustion noise, and this is shown in Figure 10(b) and (c).

The combustion noise level (CNL) comprises SA and the CPL in equation (4). The SA is specific and constant for the test engine, and the changes in combustion noise would be caused by the CPL. Figure 11(a) plots the CPL for the three-stage HTHR combustion and the three sets of two-stage HTHR combustions, $Twin_{1-2}$, $Twin_{1-3}$, and $Twin_{2-3}$. The frequency around 850−1150 Hz of $Twin_{2-3}$ in CPL is reduced by the reduction effect of $Twin_{1-3}$ with the addition of the one more heat release ahead of $Twin_{2-3}$; however, the amplifying frequency of $Twin_{1-3}$ is newly generated around 2000 Hz. This amplified CPL frequency is reduced by the strong reduction frequencies around 1900 Hz in $Twin_{2-3}$ and 2100 Hz in $Twin_{1-2}$, and the CPL of the three-stage HTHR combustion in condition A is totally reduced in the frequency range of 800−3000 Hz, as shown in Figure 11(b). The noise reduction by multiple fuel injection is the harmonization of amplification and reduction frequency characteristics in each two-stage combustion.

Test 2: optimization of the heat release shape for low combustion noise and high indicated thermal efficiency in three-stage HTHR combustion

In the two-stage HTHR combustion, the frequencies of noise amplification and reduction achieved with the interferences appear in a cyclic manner, and the NCS effect was small because of the noise amplification. However, the noise amplification can be reduced with the increase in the number of fuel injections, one example is the three-stage HTHR combustion as mentioned above.

Figure 12 suggests the optimum shapes of heat release and rate of pressure rise for the higher indicated

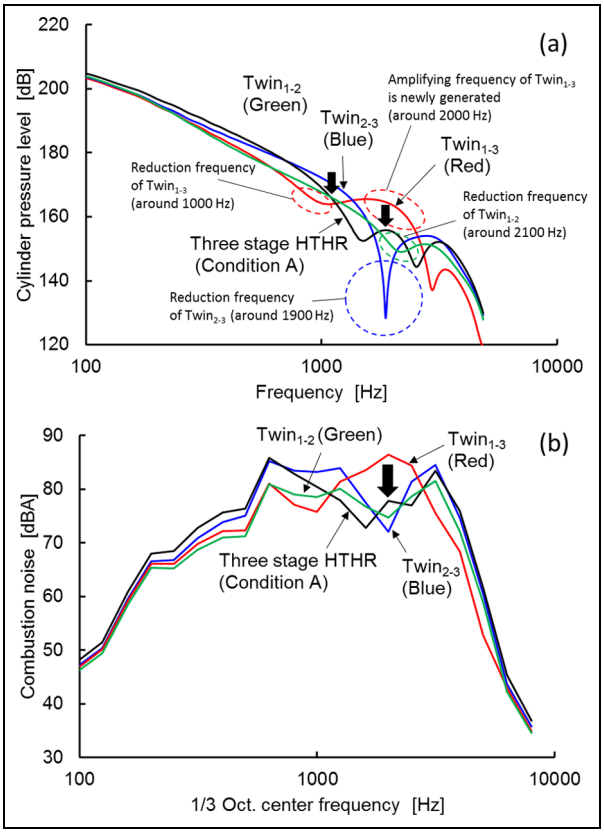

Figure 11. (a) Cylinder pressure levels and (b) frequency characteristics of the three-stage HTHR combustion and the three sets of two-stage HTHR heat releases: $Twin_{1-2}$, $Twin_{1-3}$, and $Twin_{2-3}$.

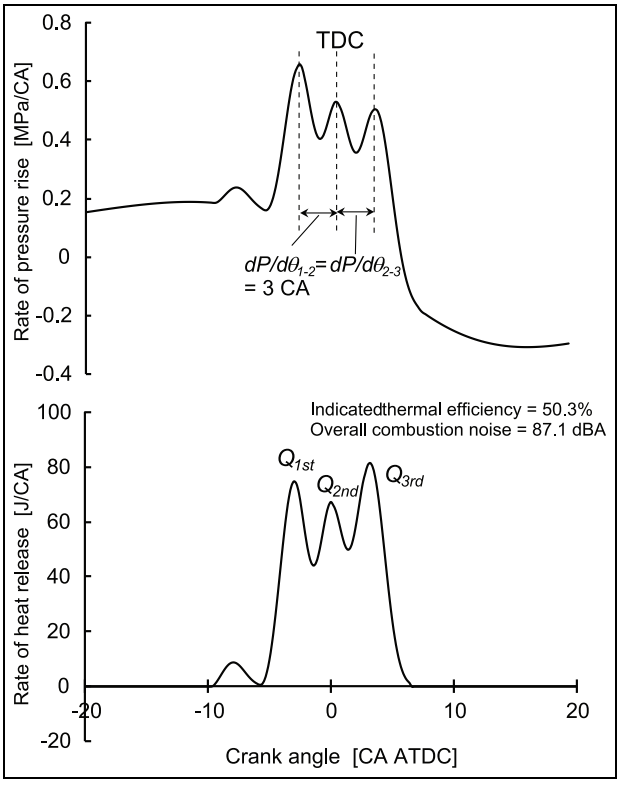

Figure 12. Optimum shapes of heat release and rate of pressure rise for the higher indicated thermal efficiency and lower combustion noise in the three-stage HTHR combustion.

thermal efficiency and the lower combustion noise in the three-stage HTHR combustion obtained by the combustion noise simulation in Test 2. The optimum heat release conditions are

1. $dP/d\theta_{1-2} = dP/d\theta_{2-3} = 3\text{CA}$
2. $Q_{1st} : Q_{2nd} : Q_{3rd} = 195\text{J} : 155\text{J} : 235\text{J}$

The resulting indicated thermal efficiency and OA are 50.3% and 87.1 dBA, respectively, and there is a 9.3 dBA combustion noise reduction compared with the pre-mixed diesel engine combustion by a single fuel injection. Figure 13 shows the effects of the heat releases of the Q_{1st}, Q_{2nd}, and Q_{3rd} ($Q_{3rd} = 585\,\text{J} - Q_{1st} - Q_{2nd}$) on the indicated thermal efficiency and OA in the $dP/d\theta_{1-2}$ and $dP/d\theta_{2-3} = 3$ CA condition. There are only small differences in the indicated thermal efficiency (top panel) because the degree of constant volume is high in all cases; however, the OA (bottom panel) changes. Each of the curves has a minimum value of OA against Q_{1st}, the Points A-F. If the Q_{1st} is on the side lower than the minimum point (left in the figure), the combustion noise becomes louder caused by the maximum rate of pressure rise of Q_{3rd}, and if the Q_{1st} is on the side higher than the minimum point (right

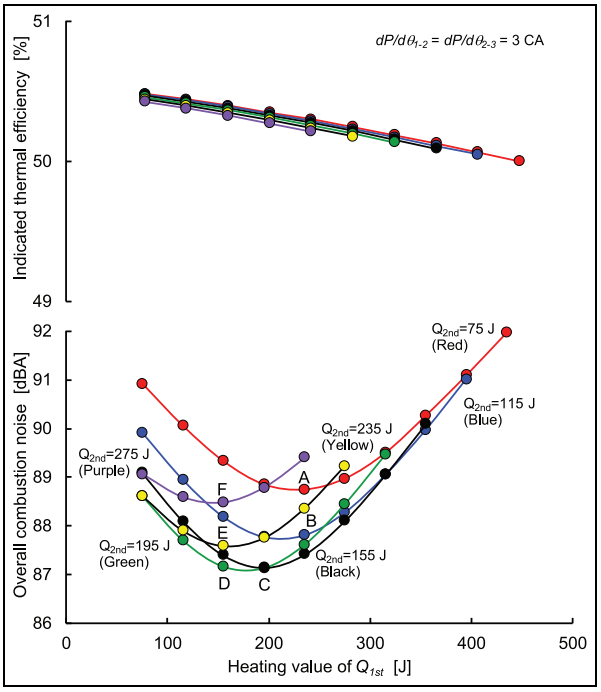

Figure 13. Effect of Q_{1st} on the indicated thermal efficiency and overall combustion noise.

in the figure), it becomes louder caused by the maximum rate of pressure rise of Q_{1st}. The Points A-F are the balancing positions for the maximum rate of

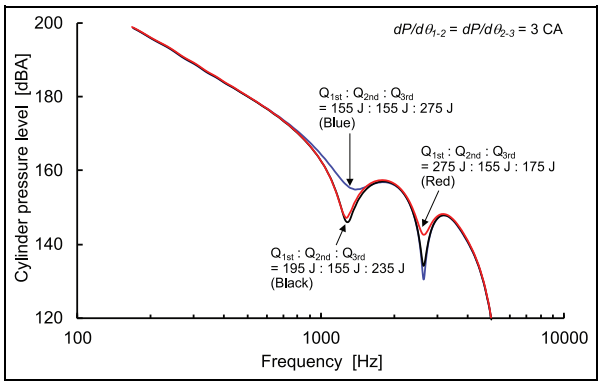

Figure 14. Effects of Q_{1st} and Q_{3rd} on cylinder pressure level (CPL).

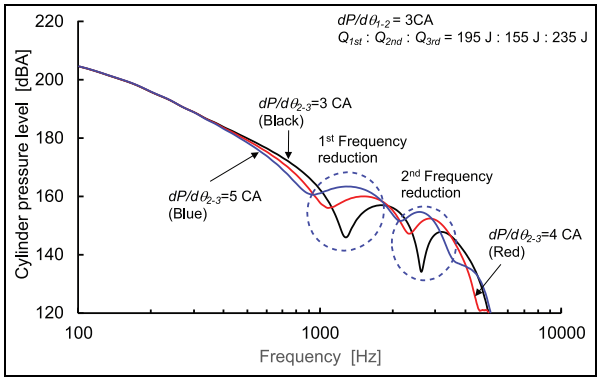

Figure 15. Effects of $dP/d\theta_{2-3}$ on cylinder pressure level.

pressure rises of Q_{1st} and Q_{3rd}, and the combustion noise becomes lowest here. Furthermore, when the Q_{2nd} is 155 J, the combustion noise curve reaches the lowest point of the six curves, and Point C suggests the lowest combustion noise point calculated by the combustion noise simulation.

Figure 14 shows the effects of Q_{1st} and Q_{3rd} on the CPL in $dP/d\theta_{1-2} = dP/d\theta_{2-3} = 3$ CA condition. When Q_{1st}:Q_{2nd}:Q_{3rd} = 155 J:155 J:275 J (Blue curve) or 275 J:155 J:175 J (Red curve), the CPL has only one frequency reduction point at 1250 or 2650 Hz; however, when Q_{1st}:Q_{2nd}:Q_{3rd} = 195 J:155 J:235 J (Black curve), it has two frequency reduction points at both 1250 and 2650 Hz.

Figure 15 shows the effects of the length of time in crank angles between the peaks of the rate of pressure rise in peaks 2 and 3 ($dP/d\theta_{2-3}$) on the CPL in Q_{1st}:Q_{2nd}:Q_{3rd} = 195 J:155 J:235 J and $dP/d\theta_{1-2} = 3$ CA condition. The CPL has two frequency reduction points and the reduction becomes stronger with the decrease in $dP/d\theta_{2-3}$. When the $dP/d\theta_{2-3} = 3$ CA, the NCS effect is the strongest of the three.

These are the reasons why the combustion noise is the lowest at Point C in Figure 13 (Q_{1st}:Q_{2nd}:Q_{3rd} = 195 J:155 J:235 J and $dP/d\theta_{1-2} = dP/d\theta_{2-3} = 3$ CA condition).

Test 3: introduction of the GA method to validate the optimized heat release shape of the three-stage HTHR combustion in Test 2

In Test 2, the calculation of the optimized heat release shape was conducted only when the crank angle at the peak heat release in the second fuel injection was at TDC. The first heat release and third heat release occur during the compression and expansion strokes, respectively, and the calculations were conducted only in this limited variable range. Furthermore, the preparations for the calculations of the combustion noise simulation are time consuming and laborious. To compensate for these shortcomings of the combustion noise simulation, the GA method was introduced and the calculation

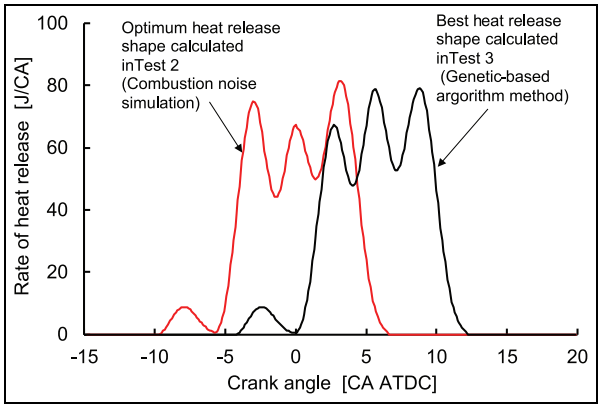

Figure 16. Comparison of heat releases calculated in Test 2 (Combustion noise simulation, red) and Test 3 (the GA method, black).

could be conducted for various conditions in a much shorter time. The crank angle of the peak heat release in the second fuel injection can also be included as one of the variable parameters, and the best heat release shape of a three-stage HTHR combustion to identify the higher indicated thermal efficiency and lower combustion noise condition was calculated. (Details of the GA are described in Appendix 2.)

The calculated results for Test 2 (Combustion noise simulation) and Test 3 (GA method) are plotted together in Figure 16, and the heat release characteristics of the LTHR, Q_{1st}, Q_{2nd}, and Q_{3rd} calculated in Test 2 and Test 3 are listed in Table 3. The calculations with the GA method was conducted 10 times until the score in equation (7) does not change over 100 generations, and the calculated result of the final generation was considered to be the answer with the GA method. In Test 2, the crank angle of the peak heat release in the second fuel injection was fixed at TDC and the heat release shape is TDC axial symmetric; however, the HTHR calculated by the GA method in Test 3 occurs after the TDC, because the restraint of the conditions for the crank angle positions of Q_{1st}, Q_{2nd}, and Q_{3rd} were less strict. The degree of constant volume in Test 2 is 99.6%, which is

Table 3. Heat release characteristics of LTHR, Q_{1st}, Q_{2nd}, and Q_{3rd} calculated in Tests 2 and 3.

	LTHR				First heat release in HTHR (Q_{1st})			
	Heating value (J)	Start of combustion (CA ATDC)	Combustion duration (CA)	Parameter M in Weibe	Heating value (J)	Start of combustion (CA ATDC)	Combustion duration (CA)	Parameter M in Weibe
Test 2	19	–9.7	4.7	1.5	195	–5.8	5.9	2.15
Test 3	19	–4.2	4.7	1.5	175	–0.1	5.9	2.15
	Second heat release in HTHR (Q_{2nd})				Third heat release in HTHR (Q_{3rd})			
	Heating value (J)	Start of combustion (CA ATDC)	Combustion duration (CA)	Parameter M in Weibe	Heating value (J)	Start of combustion (CA ATDC)	Combustion duration (CA)	Parameter M in Weibe
Test 2	155	–2.5	5.3	2.2	235	0.1	6.5	2.1
Test 3	181	3.1	5.3	2.2	228	5.7	6.5	2.1

LTHR: low temperature heat release; HTHR: high temperature heat release.

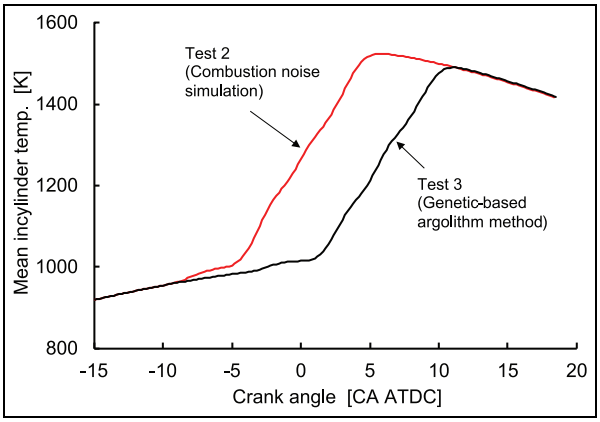

Figure 17. Plots of crank angle versus mean in-cylinder temperature for Test 2 (Combustion noise simulation) and Test 3 (the GA method).

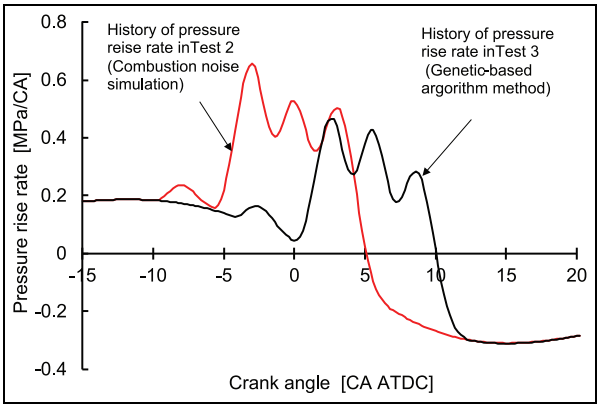

Figure 18. Plot of the pressure rise rates calculated in Test 2 (Combustion noise simulation) and Test 3 (the GA method).

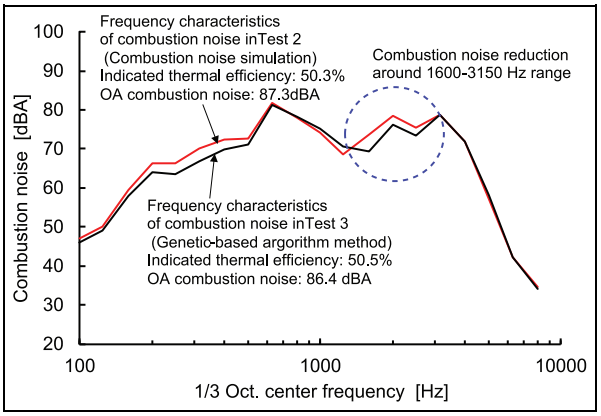

Figure 19. Frequency characteristics of the combustion noise calculated in Test 2 (Combustion noise simulation) and Test 3 (the GA method).

0.48% higher than that of Test 3; however, the combustion temperature of Test 3 near the TDC is lower than that of Test 2, as shown in Figure 17. As a result, the heat loss from the cylinder wall and exhaust emissions of Test 3 is lower than that of Test 2, and the indicated thermal efficiency of Test 3 (50.5%) is 0.2% higher than that of Test 2 (50.3%).

Figures 18 and 19 show the histories of the pressure rise rate and frequency characteristics of the combustion noise in Tests 2 and 3. In Figure 18, the combustion in Test 3 occurs in the expansion stroke and the rate of pressure rise in Test 3 is lower than that in Test 2 over the whole of the combustion duration. The combustion noise in Test 3 is lower around the 1600−3150 Hz range, which is one of the high combustion noise frequencies of the engine, as shown in Figure 19.

The OA and indicated thermal efficiency of Test 3 calculated by the GA method were 86.4 dBA and 50.5%, 0.7 dBA lower combustion noise and 0.2% higher indicated thermal efficiency than those of Test 2 calculated by the combustion noise simulation.

Table 4. Heat release characteristics of LTHR, Q_{1st}, Q_{2nd}, Q_{3rd}, Q_{4th}, and Q_{5th} in Test 4.

Number of injection	Low temperature heat release (LTHR)				First heat release in HTHR (Q_{1st})			
	Heating value (J)	Start of combustion (CA ATDC)	Combustion duration (CA)	Parameter M in Weibe	Heating value (J)	Start of combustion (CA ATDC)	Combustion duration (CA)	Parameter M in Weibe
1	19	–3.4	4.7	1.5	585	0.7	10.0	2
2		–4.6			275	–0.5	10.0	2
3		–6.3			163	–2.2	10.0	2
4		–7.6			114	–3.5	10.0	2
5		–8.8			79	–4.7	10.0	2
Number of injection	Second heat release in HTHR (Q_{2nd})				Third heat release in HTHR (Q_{3rd})			
	Heating value (J)	Start of combustion (CA ATDC)	Combustion duration (CA)	Parameter M in Weibe	Heating value (J)	Start of combustion (CA ATDC)	Combustion duration (CA)	Parameter M in Weibe
1	–	–	–	–	–	–	–	–
2	310	5	10.0	2	–	–	–	–
3	220	2.8	10.0	2	202	7.8	10.0	2
4	156	1.2	10.0	2	173	5.6	10.0	2
5	115	–0.4	10.0	2	135	3.6	9.8	2
Number of injection	Fourth heat release in HTHR (Q_{4th})				Fifth heat release in HTHR (Q_{5th})			
	Heating value (J)	Start of combustion (CA ATDC)	Combustion duration (CA)	Parameter M in Weibe	Heating value (J)	Start of combustion (CA ATDC)	Combustion duration (CA)	Parameter M in Weibe
1	–	–	–	–	–	–	–	–
2	–	–	–	–	–	–	–	–
3	–	–	–	–	–	–	–	–
4	142	10.2	10.00	2	–	–	–	–
5	142	7.6	10.00	2	114	11.9	10.0	2

LTHR: low temperature heat release; HTHR: high temperature heat release.

Test 4: optimum number of fuel injections and heat release shape for lower combustion noise with high indicated thermal efficiency analyzed by the GA method

The GA method was applied for one to five multiple fuel injections, and the optimum number of fuel injections and heat release shape for lower combustion noise and higher indicated thermal efficiency were calculated.

Figures 20 and 21 show the optimum heat release shape and rate of pressure rise in each of five cases, and the heat release characteristics of the LTHR, Q_{1st}, Q_{2nd}, Q_{3rd}, Q_{4th}, and Q_{5th} are detailed in Table 4. The heat release shape becomes flatter, lower, and wider, and the pressure rise rate decreases with the increase in the number of fuel injections. Figure 22 shows the frequency characteristics of the combustion noise with multiple fuel injections, and the combustion noise in the 200−3000 Hz band decreases with the increase in the number of fuel injections. Figure 23 plots the pressure-volume (P-V) history in the compression and expansion strokes. With the increase in the number of fuel injections, the maximum rate of pressure rise becomes lower and the P-V curve shows constant pressure combustion in the initial stage of the expansion stroke; however, the indicated thermal efficiency decreased, as shown in Figure 24, because the degree of constant volume worsens.

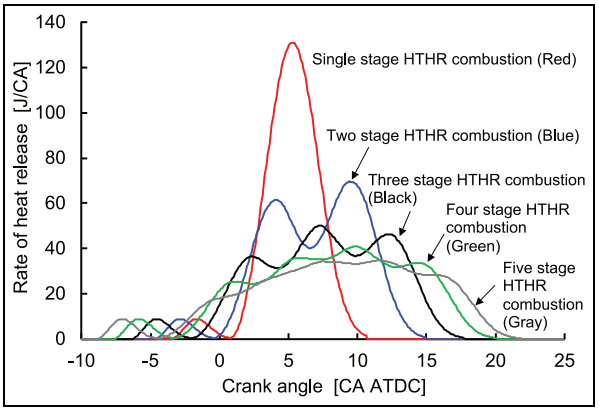

Figure 20. Optimum heat releases for one to five injections calculated by the GA method.

Conclusion

This article investigates combustion noise reduction maintaining high thermal efficiency by multiple fuel injections with numerical simulations, GA method, and

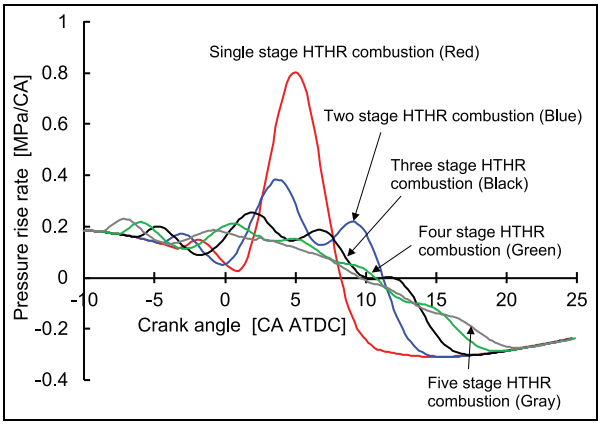

Figure 21. Pressure rise rates for one to five injections in Figure 23.

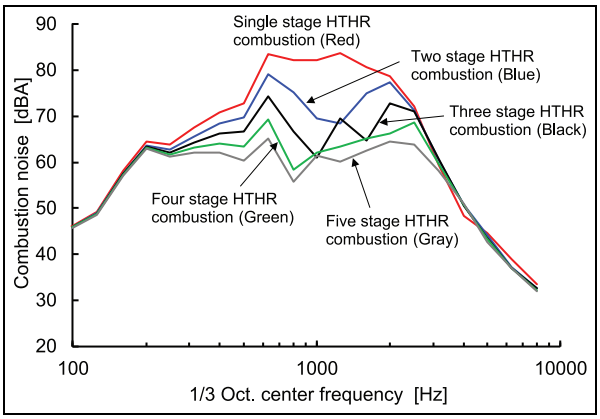

Figure 22. Frequency characteristics of combustion noise with 1−5 fuel injections.

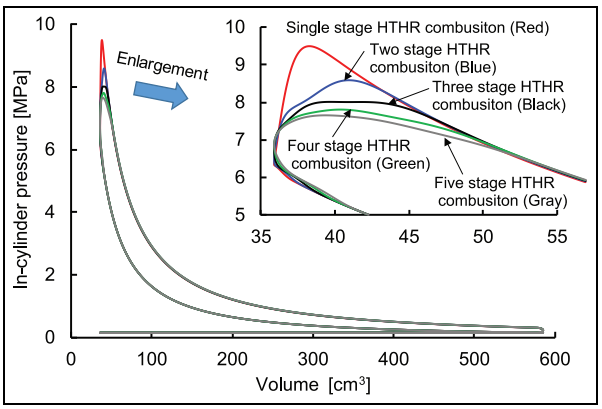

Figure 23. Pressure-volume histories (PV line) for multiple fuel injections.

engine tests. The conclusions of the investigations may be summarized as follows:

1. In the three-stage HTHR combustion, the amplified noise at 2000 Hz by $Twin_{1-3}$ is weakened by the reduction in noises around 1900−2100 Hz of $Twin_{1-2}$ and $Twin_{2-3}$, and the OA can be reduced (Test 1).
2. Figure 12 is the optimum heat release shape of three-stage HTHR combustion calculated by the combustion noise simulation. The indicated thermal efficiency was 50.3% and the combustion noise was 87.1 dBA (Test 2).

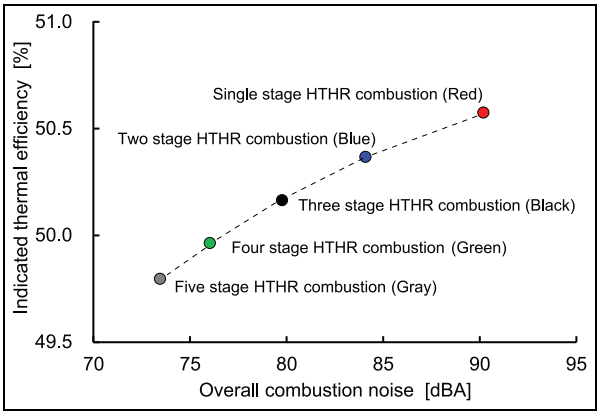

Figure 24. Overall combustion noise versus indicated thermal efficiency for multiple fuel injections.

A GA method was introduced to achieve the seedily calculations of optimum heat release shape for three to five fuel injections. The GA method was first applied to optimize the heat release shape for lower combustion noise with high indicated thermal efficiency in three fuel injections in Test 3, and the optimum number of fuel injections and heat release shape was investigated in Test 4.

3. The heat release shape calculated by GA method occurs after the TDC comparing with the calculated results of combustion noise simulation in Figure 16. The degree of constant volume decreased 0.48%; however, the lower heat loss from the cylinder wall, a 50.5% indicated thermal efficiency was achieved. Furthermore, the combustion occurs in the expansion stroke, and the combustion noise calculated by GA method was 86.4 dBA, which is 0.7 dBA lower than that of combustion noise simulation in Test 2.
4. The constant pressure and low maximum rate of pressure rise combustion after the TDC by multiple fuel injections is the most advantageous to lower the combustion noise; however, more than four injections lead to a lowering of the indicated thermal efficiency because the degree of constant volume worsens.

Declaration of conflicting interests

The author(s) declared no potential conflicts of interest with respect to the research, authorship, and/or publication of this article.

Funding

This work was supported by Council for Science, Technology and Innovation (CSTI), Cross-ministerial Strategic Innovation Promotion Program (SIP), "Innovative combustion technology" (funding agency: JST).

References

1. Murayama T, Kojima N and Satomi Y. A simulation of diesel engine combustion noise. SAE technical paper 760552, 1976.
2. Kojima N. An Evaluation of combustion noise generation in diesel engine structure. SAE technical paper 890126, 1989.
3. Komori M, Miura Y, Mikami M and Kojima N. 19 separation of combustion noise using transient noise generation model. SAE technical paper 2002-32-1788, 2002.
4. Sjoberg M and Dec J. Effects of engine speed, fueling, and combustion phasing on the thermal stratification required to limit HCCI knocking intensity. SAE technical paper 2005-01-2125, 2005.
5. Johansson T, Johansson B, Tunestal P and Aulin H. HCCI operating range in a turbo-charged multi cylinder engine with VVT and spray guided DI. SAE technical paper 2009-01-0494, 2009.
6. Scarpati J, Wikstrom A, Jonsson O and Glav R. Prediction of engine noise using parameterized combustion pressure curves. SAE technical paper 2007-01-2373, 2007.
7. Shahlari A, Hocking C and Ghandhi J. Comparison of compression ignition engine noise metrics in low-temperature combustion regimes. *SAE Int J Engines* 2013; 6(1): 541–552.
8. Shibata G, Shibaike Y, Ushijima H and Ogawa H. Identification of factors influencing premixed diesel engine noise and mechanism of noise reduction by EGR and supercharging. SAE technical paper 2013-01-0313, 2013.
9. Ozawa H and Nakajima K. Simultaneous improvement of combustion noise and fuel consumption on diesel engines. *Trans Soc Automot Eng Jpn* 2012; 43(5): 1099–1104.
10. Ozawa H and Nakajima K. Study on combustion chamber resonance with a view to improving diesel engine sound quality. *Trans Soc Automot Eng Jpn* 2015; 46(2): 425–430.
11. Okubo M and Yonezawa T. Study of method of separate engine noise sources using coherence analysis. *Trans Soc Automot Eng Jpn* 1989; 40: 152–158.
12. Shibata G, Ushijima H and Ogawa H. Combustion noise analysis of premixed diesel engine by engine tests and simulations. SAE technical paper 2014-01-1293, 2014.
13. Shibata G, Ishii K, Ushijima H and Foster DE. Optimization of heat release shape and the connecting rod crank radius ratio for low engine noise and high thermal efficiency of premixed diesel engine combustion. SAE technical paper 2015-01-0825, 2015.
14. Fuyuto T, Taki M, Ueda R, Hattori Y, Kuzuyama H and Umehara T. Noise and emissions reduction by second injection in diesel PCCI combustion with split injection. *SAE Int J Engines* 2014; 7(4): 1900–1910.
15. Ikeda H, Iida N, Kazuyama H, Umehara T and Fuyuto T. An investigation of controlling two-peak heat release rate for combustion noise reduction in split-injection PCCI engine using numerical calculation. SAE technical paper 2014-32-0132, 2014.
16. Nishi M, Ikeda H, Iida N, Kuzuyama H, Umehara T and Fuyuto T. Numerical assessment of controlling the interval between two heat-release peaks for noise reduction in split-injection PCCI combustion. SAE technical paper 2015-01-1851.
17. Shibata G, Nakayama D, Okamoto Y and Ogawa H. Diesel engine combustion noise reduction by the control of timings and heating values in two stage high temperature heat releases. *SAE Int J Engines* 2016; 9(2): 868–882.
18. Okamoto Y, Amanuma Y and Shibata G, Ogawa H and Kobashi Y. Combustion noise reduction of premixed diesel engine by changing the phase and the number of times of split heat releases with multiple fuel injections. In: *Proceedings of the 27th IC engine symposium*, Tokyo, Japan, 2016.
19. Busch S, Zha K, Miles P, Warey A, Pesce F, Peterson R and Vassallo A. Experimental and numerical investigations of close-coupled pilot injections to reduce combustion noise in a small-bore diesel engine. *SAE Int J Engines* 2015; 8(2): 660–678.
20. Busch S, Zha K and Miles P. Effect of close pilot spacing on combustion and emissions, http://www.osti.gov/scitech/servlets/purl/1241678
21. Fuyuto T and Taki M. Noise-canceling spike between pressure rise peaks of pilot and main combustion in diesel engine. In: *Proceedings of the 9th international conference on modeling and diagnostics for advanced engine systems (COMODIA 2017)*, Okayama, Japan, 25–28 July 2017, Paper no. B208.

Appendix 1

Noise reduction effects by the NCS combustion

In Figure 25, the crank angle interval of the CA10s in the first and second HTHRs is defined as the $CA10_{1-2}$, and the crank angle interval of the peaks of the maximum rate of pressure rise between the first and second fuel injections is defined as $dP/d\theta_{1-2}$. Equations (8) and (9) show the amplifying and reduction frequencies. The Δt in the equation is the interval (seconds) of $dP/d\theta_{1-2}$, and Δt equals to $(dP/d\theta_{1-2})/12{,}000$ as the engine is operated at 2000 r/min

$$Amplifying\,frequency\ :\ f_n = \frac{n_A}{\Delta t} \quad (n_A = 1, 2, 3, \ldots) \tag{8}$$

$$Reduction\,frequency\ :\ f_n = \frac{(2n_C + 1)}{2\Delta t} \quad (n_C = 0, 1, 2, 3, \ldots) \tag{9}$$

Appendix 2

Optimum number of generations and the evaluation function for the GA method

To know an optimum number of generations in the GA method, a number of calculations were conducted under the three-stage HTHR combustion condition. Equation (10) is an example of an evaluation function and a higher score with this equation means a higher

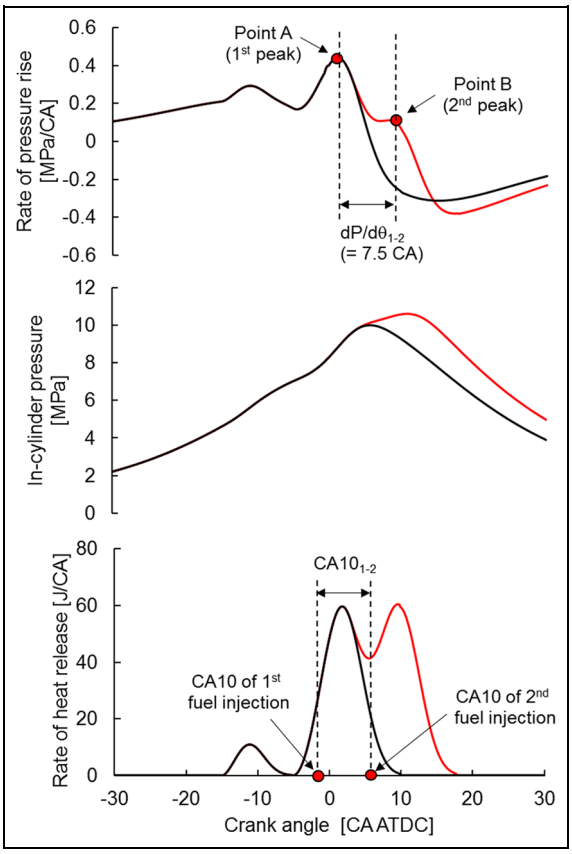

Figure 25. Definitions of $CA10_{1-2}$ and $dP/d\theta_{1-2}$ in two-stage combustion.

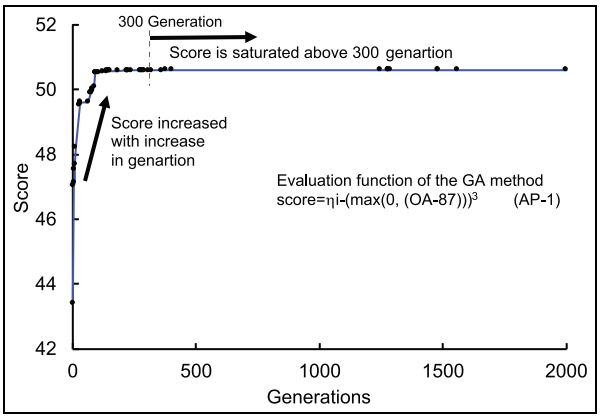

Figure 26. Score history of generation-based algorithm method against generations (equation (10)).

indicated thermal efficiency and lower combustion noise. In this case, the basic overall combustion noise (BOA) was set at 87 dBA, and if the calculated OA is lower than 87 dBA, equation (10) becomes the function of the indicated thermal efficiency

$$Score = \eta i - (max(0, (OA - BOA)))^3 \quad (10)$$

where *Score* is the score of evaluation function, ηi is the indicated thermal efficiency (%), OA is the overall combustion noise (dBA), BOA is the basic overall

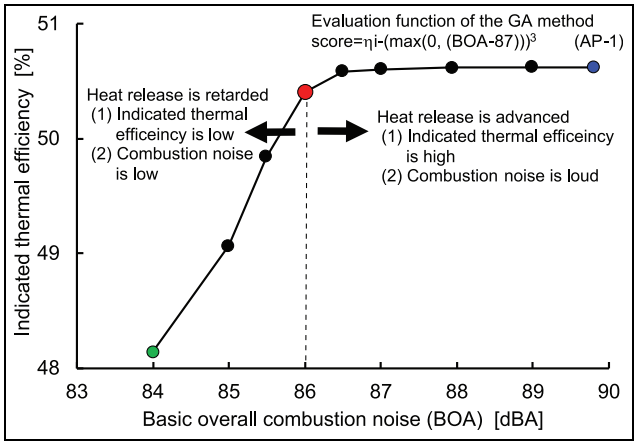

Figure 27. Plots of basic overall combustion noise versus indicated thermal efficiency (equation (10)).

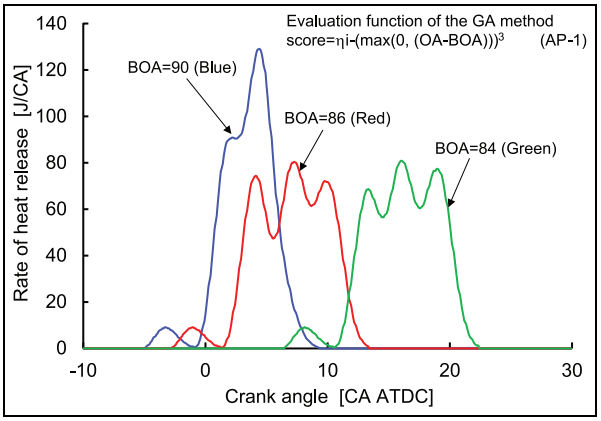

Figure 28. Optimized heat release histories for the basic overall values of 84, 86, and 90 (equation (10)).

combustion noise (87 dBA), and max (A, B): A (if A > B) or B (if A < B).

The GA calculations were conducted over 2000 generations, and Figure 26 plots the generation number versus the score. As the number of generations increases, the score increases and saturates above 300 generations in this case. In this article, the GA calculations are conducted until the score does not change over 100 generations, and the calculated result of the final generation is considered the answer with the GA method. In the GA calculation, a random number generated by the workstation computer is used, and in rare cases this results in a local solution. To avoid results with such a local solution, the GA calculations are conducted more than 10 times in one condition.

The BOA in equation (10) is varied from 90 to 84, and the GA calculations were conducted each BOA value. Figure 27 plots the BOA versus indicated thermal efficiency, and each plot is the "optimum" for the given BOA number, with the BOA 86 the critical point in this case. Figure 28 shows the optimum heat releases for three different BOA numbers, 90, 86, and 84. With the BOA < 86, the GA calculation suggests a retardation of the heat release, and the indicated thermal

efficiency is low. With the BOA $>$ 86, the heat release is advanced and the indicated thermal efficiency is high; however, the combustion noise increases. The calculation suggests that the BOA = 86 is the optimum for equation (10).

Equation (11) (the same as equation (7)) is another evaluation function for the GA method, and the 0.5% indicated thermal efficiency is equivalent to 1.0 dBA overall combustion noise

$$Score = \eta i - OA \cdot 0.5 \tag{11}$$

where *Score* is the score of evaluation function, ηi is the indicated thermal efficiency (%), and OA is the overall combustion noise (dBA).

Figure 29 plots the OA versus score with equation (11), and the score is the highest when the combustion noise is 86, corresponding to the BOA = 86 in equation (10), and equation (11) was used as the evaluation function for the GA method in this article.

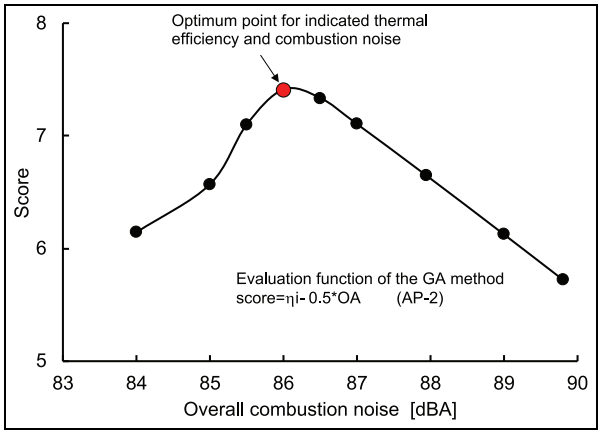

Figure 29. Plots of overall combustion noise versus score (equation (11)).